Analysis of the effect of medium and membrane conductance on the amplitude and kinetics of membrane potentials induced by externally applied electric fields

Zenobia Lojewska, Daniel L. Farkas, Benjamin Ehrenberg, and Leslie M. Loew
Department of Physiology, University of Connecticut Health Center, Farmington, Connecticut 06032

ABSTRACT The kinetics and amplitudes of membrane potential induced by externally applied electric field pulses are determined for a spherical lipid bilayer using a voltage-sensitive dye. Several experimental parameters were systematically varied. These included the incorporation of gramicidin into the membrane to alter its conductivity and the variation of the external electrolyte conductivity via changes in salt concentration. The ability of the solution to Laplace's equation for a spherical dielectric shell to quantitatively describe the membrane potential induced on a lipid bilayer could thus be critically evaluated. Both the amplitude and the kinetics of the induced potential were consistent with the predictions of this simple model, even at the extremes of membrane conductance or electrolyte concentration. The success of the experimental approach for this system encourages its application to more complex problems such as electroporation and the influences of external electric fields in growth and development.

INTRODUCTION

Applied and endogenous electric fields can significantly influence cellular physiology. Depending on the cell type and the field strength, these effects can be either slow and subtle or rapid and striking. Some of the subtle effects which have been established include influences on growth and development (Jaffe and Poo, 1979; Robinson, 1985; Goldsworthy, 1986), bone healing (Singh and Katz, 1986), and reorganization of cell surface molecules (Poo, 1981; Lin-Liu, et al., 1984; Ryan et al., 1988). These effects usually require low to moderate fields of sustained duration and can take hours to days to become manifest. The responses which might be classified as fast can include membrane permeabilization (e.g., Knight and Baker, 1982; Tsong, 1983; Neumann et al., 1988), cell or vesicle fusion (e.g., Zimmermann, 1982; Nea et al., 1987; Bates et al., 1983), activation of membrane-bound ATPases (Tsong, 1983; Vinkler et al., 1982; Kagawa and Hamamoto, 1986), and the triggering of action potentials (recent examples: Obaid et al., 1985; Chan and Nicholson, 1986). Whereas the subtle responses are no less important, these latter effects are characterized by rapid and dramatic changes after short ($\leq$1 ms) field pulses.

Many of these responses to external electric fields have been tied, either by inference or direct experimental evidence, to the induced changes in membrane potential along the cell surface. These conclusions arise from solutions to Laplace's equation for a dielectric shell, of thickness, d, and capacitance, C_m, in a conducting medium exemplified by an approximate solution for the time-dependent membrane potential, $V_m(t)$, induced by a uniform electric field, E, for the proverbial spherical geometry.

$$\frac{V_m(t)}{d} = \frac{3(R/d)[1 - e^{-(2t\lambda_0/3RC_m)(1+3R\lambda_m/2d\lambda_0)}]E\cos\theta}{2 + 3(R\lambda_m)/(d\lambda_0)}. \quad (1)$$

Eq. 1 is somewhat simplified compared with the exact solution (cf. Ehrenberg et al., 1987) by assuming that R, the sphere radius, is much larger than d (this assumption is certainly accurate for cells but may not be for vesicles) and that the internal and external media have the same conductivities, λ_0. We do not include the usual additional assumption that the membrane conductivity, λ_m, is insignificant compared with λ_0. For cases involving electroporation or analysis of channel-containing membranes, explicit consideration of λ_m is clearly necessary. The angle θ is between the field direction and the normal to the surface of the sphere at the point where V_m is being calculated. For a 10-μm spherical cell in normal physiological saline, the amplification amounts to $\sim 3 \times 10^3$ at the poles facing the electrodes (hyperpolarization in the cathodic hemisphere and depolarization in the anodic hemisphere) and the exponential time constant for the development of this membrane potential is in the nanosecond domain. Qualitatively this can be understood as a simple RC circuit comprised of an effective capacitance for the membrane and the resistance of the medium surrounding it.

Dr. Ehrenberg's permanent address is Department of Physics, Bar Ilan University, Ramat Gan 52 100, Israel.

Thus, the qualitative conclusions of the theory—amplification of the field in the membrane and rapid induction of the potential—have been used to rationalize some of the complex cellular phenomena elicited by electric fields. However, a detailed quantitative experimental examination of how well the theory holds for a lipid bilayer membrane has not been undertaken until quite recently. The spatial variation of the membrane potential in spherical and ellipsoidal cells has been experimentally investigated in a study employing digital video microscopy and a voltage-sensitive dye (Gross et al., 1986); the essential result was that the angular dependence and the amplitude of the potential matched the predictions of Eq. 1 quite well. This was actually the first study to demonstrate the validity of the spatial component of the theory for biological membranes.

The time-dependent component of the theory had been previously addressed by analyzing the kinetic details of electrophotoluminescence from photosynthetic blebs (Farkas et al., 1984). It was shown that Eq. 1 could nicely rationalize the experimental results from this intrinsic probe. More recently, we reported preliminary results in this journal (Ehrenberg et al., 1987) showing that the dye methodology could also be used to quantitatively monitor the kinetics of the development of a membrane potential following the onset of an external electric field. The extrinsic probe methodology has the advantage over electrophotoluminescence that it is general (i.e., not confined to chloroplast membranes), requires simpler and more readily available equipment, and can be analyzed and interpreted in a more straightforward way.

This paper is an elaboration of the work reported by Ehrenberg et al. (1987). We use potentiometric dye fluorescence instead of transmittance to determine, simultaneously, the amplitude and the time course of the field-induced membrane potential for the spherical bilayer. Using this method, we probe some of the more subtle features of Eq. 1, including its ability to account for the presence of highly conducting channels in the membrane. We show that the theory, derived for a macroscopic dielectric shell in a uniform conductor, is able to quantitatively account for the behavior of a lipid bilayer over a wide range of electrolyte concentrations and membrane conductivities.

METHODS

Materials

1-(3-Sulfonatopropyl)-4-[β][2-(di-*n*-butylamino)-6-naphthyl vinyl] pyridinium betaine (di-4-ANEPPS) was prepared according to Hassner et al. (1984). Di-4-ANEPPS was dissolved in ethanol (analytical grade, Aldrich Chemical Co., Milwaukee, WI) at 3 mM concentration. Gramicidin D (mol wt 1,880) was obtained from Sigma Chemical Co., St. Louis, MO, and stored at 4°C as stock solutions in ethanol. Cholesterol was obtained from Sigma Chemical Co., octane from Aldrich Chemical Co. (high purity grade "Gold Label") to prepare oxidized cholesterol (Tien, 1974), which was found to be the only lipid, in our hands, capable of producing sufficiently long-lived spherical lipid bilayer (SLB). Octane was removed from the supernatant resulting from Tien's procedure, and the oxidized cholesterol redissolved in decane (Aldrich Chemical Co., "Gold Label") at 30 mg/ml. KCl solutions (concentration range, 0.04–100 mM) were prepared from double distilled deionized water and their conductivity determined with an impedance bridge (model 1650-B, General Radio Inc., Concord, MA). All solutions were stored under refrigeration until used.

Membrane formation

SLBs were suspended in the KCl solution from a Teflon tube. The tube was machined with inner and outer diameters of 1 and 4 mm, respectively. At the end supporting the bilayer, a 0.5-mm-deep groove helped accommodate the excess lipid and solvent resulting from membrane thinning, thus increasing membrane stability. The other end was machined to fit the Luer tip of a micrometer syringe. The Teflon tube was filled with KCl solution at the desired concentration, the end painted with a small amount of membrane-forming solution and the tip lowered into a cuvette of the same KCl solution which also contained di-4-ANEPPS (0.3 μM) and had been filtered through a polycarbonate membrane (Bio-Rad Laboratories, Richmond, CA; pore size, 0.8 μm). A SLB was then formed by applying hydrostatic pressure with the micrometer syringe and allowing the lipid bubble thus formed to thin to bilayer thickness. The bubbles were essentially spherical except for the upper $\approx$20% of the surface covered by the Teflon tip. The bathing solution was stirred with a small magnetic stirrer and the thinning process was usually complete within 15 min, as could be ascertained optically and electrically.

The measurement of the SLB radius (R) was achieved by determining the displacement needed to bring opposite poles of the SLB into the light beam on the micrometer of the micromanipulator. These measurements could be checked via the calibrated reticle on the viewing stereomicroscope.

Optical determination of induced membrane potential

The system employed in this laboratory for characterizing potential sensitive dyes (Loew, 1982; Loew and Simpson, 1981; Fluhler et al., 1985) was modified for these experiments (Fig. 1). A pair of parallel Pt electrodes were fit into the 1-cm sides of a 2 × 1 × 4 cm glass cuvette via Teflon spacers along the cuvette floor. A square wave generator model 3010, (B K Precision, Dynascan Corp., Chicago, IL) served to supply an external electric field to the system via these electrodes. To measure the kinetics of the development of the membrane potential induced on a spherical bilayer by the external electric field, the relative transmittance change ($\Delta T/T$) and/or relative fluorescence change ($\Delta F/F$) of di-4-ANEPPS were followed.

A 100-W tungsten-halogen lamp (Xenophot, HLX 64625, Osram Co., Berlin, FRG) powered by a stabilized DC source (JQE 0–15 V, 0–12 A; Kepco, Brooklyn, NY) was focused onto the 2-mm entrance slit of a monochromator (Jobin-Yvon, France). The exit slit of the monochromator was modified to provide 1 × 2 mm emerging light beam which was focused onto a small patch of the SLB perpendicular to the direction of the external field with a 10× achromat objective; the beam width at focus was $\approx$0.2 mm. Transmitted light was collected by a matching objective and detected with a photodiode (model PIN 10/UV 4455, United Detector Technology, Inc., Santa Monica, CA). The incident wavelength for transmittance and fluorescence measurements was set at

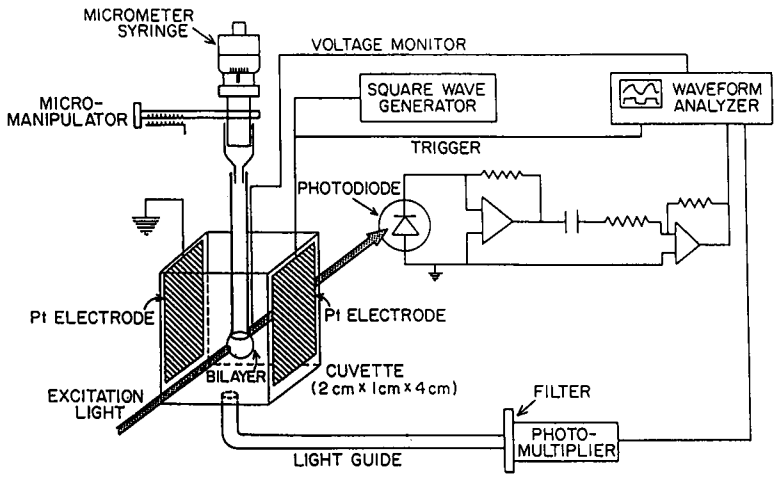

FIGURE 1 Experimental arrangement for measuring the membrane potential induced by an external electric field across a spherical lipid bilayer. Light from a monochromator is focused on one side of the SLB, illuminating a small area (pole) closest to the external field electrode. The transmitted light is measured with a photodiode and fluorescence detected via fiber optics mounted under the cuvette leading to a photomultipler. AC-coupled signals are sent to the waveform analyzer.

544 nm (see relative transmittance response and relative fluorescence excitation spectra of di-4-ANEPPS, Fluhler et al., 1985). Fluorescence was detected at >610 nm (cut-off filter, model RG-610, Schott Glass Technologies Inc., Duryea, PA) via a fiber optic mounted under the cuvette leading to a photomultiplier (model 9781R, EMI-Gencom Inc., Plainveiw, NY) followed by a current-sensitive preamplifier (model 181, EG&G Princeton Applied Research Corp., Princeton, NJ) The entire optical system was mounted on a 1-m optical rail and connected to a vibration-damping optical table (Newport Corp., Fountain Valley, CA).

Total fluorescence, F, and total transmittance were determined with a digital voltmeter or an oscilloscope (model 7904, Tektronix Inc., Beaverton, OR). The ac components of the transmitted light signal was amplified 100 fold with the amplifying unit of the oscilloscope. The differential signals could be detected either with a lock-in amplifier (model 5203, Princeton Applied Research Corp.) or by signal averaging with a waveform analyzer (model 6000, Data Precision, Danver, MA) equipped with either a 100 KHz or 100 MHz amplifier module (models 610 or 620, respectively). A reference signal for the lock-in amplifier and trigger for the waveform analyzer was supplied by the function generator or by a Pt probe electrode (Pt wire, 0.5 mm in diameter) attached to the Teflon tip on which the SLB was formed and suspended in the bathing solution just above the bubble. The total fluorescence signal was corrected for background so that only the membrane-bound dye fluorescence was used to calculate $\Delta F/F$. The averaged optical signals were transferred from the waveform analyzer to an Apple II Plus computer via an RS 232 interface for storage on floppy disk and data analysis, or directly plotted on a model 7225A digital plotter (Hewlett-Packard Co., Palo Alto, CA).

Measurements of membrane resistance

One Ag/AgCl electrode, ~3 cm long and 1 mm in diameter, was placed in the cuvette as close as possible to the bubble to minimize the interposed bathing solution resistance. The second electrode, 0.25 mm in diameter, was placed inside the Teflon tip, reaching to near its end. Knowing the total voltage applied to the system from the square wave generator and voltage drop across a fixed known resistance in series we were able to calculate the resistance between the Ag/AgCl electrodes. The resistance of the membrane alone was determined by subtracting the electrode and salt solution resistance measured after the bubble was broken.

To minimize errors due to Ag/AgCl electrode polarization, bipolar square voltage pulses were applied; it is important that the stimulus pulse be wide enough to fully charge the membrane capacitance to a steady value and eliminate the effect of membrane capacitance from the measurements.

RESULTS

Fluorescence and transmittance responses to membrane potential

The fast potentiometric probe di-4-ANEPPS was used to measure the potential induced by a train of external electric field pulses on a spherical lipid membrane. We have employed this probe because it is fast, insuring a faithful record of the time course for the development of the induced potential and because its sensitivity, ≈9% fluorescence change per 100 mV membrane potential change, is the largest for any fast dye we have tested for the SLB (Fluhler et al., 1985). The fluorescence of this dye was used in previous investigations of membrane potentials induced by electric fields applied to cells (Gross et al., 1986; Ehrenberg et al., 1987), and the sensitivity of the dye coincided with the electrode calibration on the voltage clamped SLB obtained by Fluhler et al. (1985).

Although transmittance measurements are technically somewhat easier, we chose to also determine fluorescence changes because of the quantitative correlation between relative fluorescence changes and membrane potential.

Thus, with the fluorescence response, both the time course and the amplitude of the induced membrane potential is obtained. Also, with our optical system, the fluorescence mode gave better signal-to-noise ratios.

The amplitude of the induced membrane potential was calculated from the preexponential part of Eq. 1 and plotted against the relative fluorescence change $\Delta F/F$ in Fig. 2. The relative fluorescence change is linear in this calculated membrane potential. The slope of 9%/100 mV is identical to that obtained for the voltage clamped SLB (Fluhler et al., 1985). In other words, the membrane potentials calculated from Eq. 1 are experimentally verified by the fluorescence response of this well-calibrated dye.

Very high external applied fields would result in loss of linearity, reflecting dielectric breakdown of the membrane. Therefore in our experiments we chose external field strengths such that the induced membrane potentials would not exceed ±300 mV. The linearity of the relative transmittance change with membrane potential was reported in our previous paper (Ehrenberg et al., 1987). It should be emphasized that a linear dependence of the dye response on membrane potential is a necessary condition, if one is to use the response to measure the kinetics of the development of this potential.

Fig. 3 shows the optically detected time course of the membrane potential when a 340-Hz bipolar square wave of 0.75 V/cm amplitude was applied to a bubble of 4 mm diameter in 5 mM KCl solution. Both optical signals rise

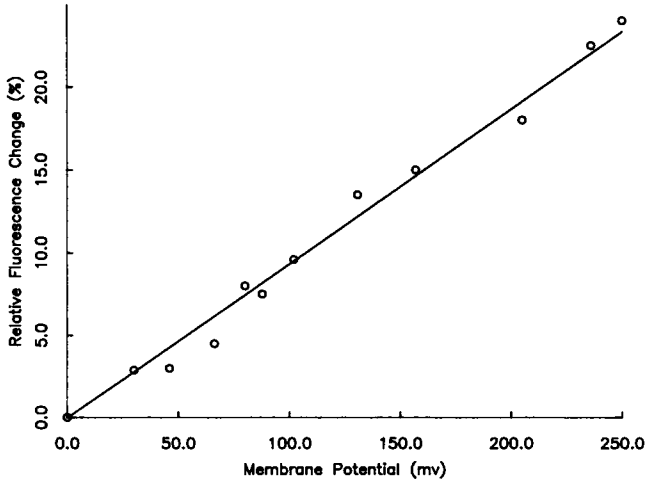

FIGURE 2 Linearity of the dye response (fluorescence) with membrane potential. V_m was calculated from the steady-state form of Eq. 1 at θ = 0° or 180°, assuming $\lambda_0 \gg \lambda_m$. KCl concentration, 5 mM; di-4-ANEPPS concentration, 0.3 μM. The results are quite insensitive to the positioning of the beam; it would have to be off the poles of the SB by 26° to give a 10% error.

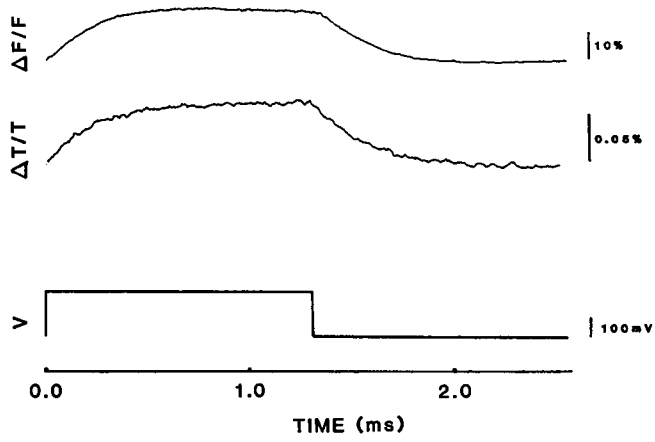

FIGURE 3 Membrane potential induced across the spherical bilayer, monitored by transmittance and fluorescence changes. Conditions: 0.3 μM di-4-ANEPPS, 5 mM KCl, data acquisition at 5 μs/point, average of 10,000 sweeps, radius R (SLB) = 2 mm. (*Bottom trace*) Applied voltage profile, corresponding to ± 120 mV in the illuminated area. (*Middle trace*) Relative transmittance change ($\Delta T/T$). (*Top trace*) Relative fluorescence change ($\Delta F/F$).

with a single exponential as predicted by Eq. 1; the time course of the transmittance change and fluorescence change obtained from an exponential fit to the data were essentially the same. The fact that a single exponential suffices to describe the kinetics indicates that second order effects such as electrostriction do not cause significant deviations from Eq. 1.

External field–induced membrane potential is attenuated in a predictable way by high membrane conductance

In this paper the experiments have been designed to quantitatively examine cases where the membrane conductance λ_m cannot be neglected. Gramicidin was chosen to modulate λ_m because it easily incorporates to produce a cation channel which has been extensively characterized in the literature (for review see Andersen, 1984).

Thus, upon introduction of gramicidin to the bilayer the amplitude, $\Delta F/F$, and the rise time, t, of the fluorescent signal decreased in a self-consistent manner as a function of membrane conductivity (Fig. 4). The relative fluorescence signals were recorded for gramicidin concentrations of 0, 0.1, 0.25, 1, 2.5, 5, 10, and 20 μM in the outer bathing solution. As predicted by Eq. 1, the rise times and relative amplitudes decrease by approximately the same factor with increasing λ_m. We noticed no futher changes in rise time or amplitude when gramicidin concentration in the bathing solution exceeded 5 μM. This

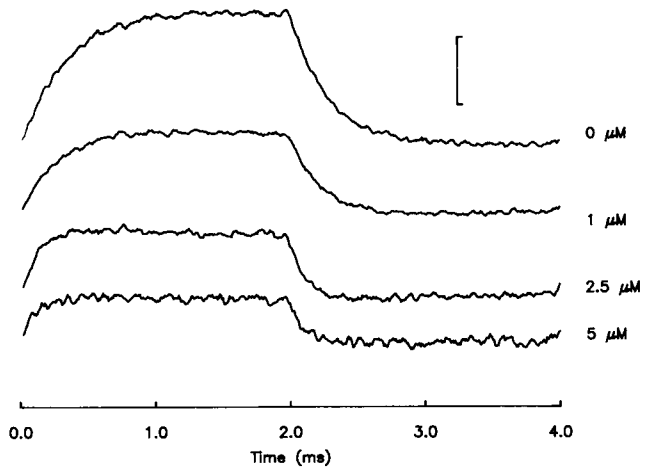

FIGURE 4 Time course and amplitude of electric field–induced fluorescence change upon modulation of membrane conductivity with gramicidin. Added gramicidin concentrations are shown for each trace. Rise times and amplitudes change by roughly the same factor, as theoretically expected. Conditions: 5 mM KCl, $V = \pm 120$ mV. Vertical bar indicates 10% relative fluorescence change.

could be due to membrane saturation with gramicidin channels.

The values for the induced membrane conductivity λ_m upon addition of gramicidin were extracted from Eq. 1 using either the changes in the rate constant t^{-1} or the amplitude of relative fluorescence, $\Delta F/F$:

$$\lambda_m = \frac{2d\lambda_0}{3R_G}\left[\frac{t_G^{-1} \cdot R_G}{t_N^{-1} \cdot R_N} - 1\right]$$

$$\lambda_m = \frac{2d\lambda_0}{3R_G}\left[\frac{(\Delta F/F)_N \cdot R_G}{(\Delta F/F)_G \cdot R_N} - 1\right],$$

where the subscripts N and G indicate the absence and presence of gramicidin, respectively. The ratio of the bubble radius measured for a particular gramicidin concentration, R_G, to the average value of the radius for determinations made without gramicidin, R_N, has been inserted in the expressions to normalize for variations in bubble size from experiment to experiment. This was necessary because it proved very difficult to introduce gramicidin to the solution bathing a preformed SLB without breaking it; thus, some measurements of the fluorescence responses with and without a given concentration of gramicidin had to be performed on different SLBs.

Multiple determinations of λ_m were thus obtained from both the amplitude and the kinetics of the fluorescence response at each gramicidin concentration. The average of these values at each concentration were then fit to a one-site saturable binding model via a weighted nonlinear least-square analysis.

$$\lambda_m(c) = \frac{[\lambda_m(\infty) - \lambda_m(0)] \cdot c}{c + K_d/n} + \lambda_m(0),$$

where $\lambda_m(c)$ is the membrane conductivity at the gramicidin concentration in the bathing solution equal to c, and K_d/n is the single-site binding constant per number of binding sites. The parameter K_d/n serves as a measure of the gramicidin binding to the membrane and was found to be 1.43 μM = 2.69 μg/ml. The binding curve is displayed in Fig. 5 along with the data. Note that the same curve is shown in the top and bottom of Fig. 5 and was generated by fitting the averaged conductivities derived from both the kinetic and amplitude measurements; the data derived from the kinetic and amplitude measurements are separately displayed, however. Whereas, this has the effect of making the fit look worse than it really is, we felt it important to show that the two sets of data are largely self consistent.

Direct electrical measurements of the membrane resistance (and thus, the specific conductivity λ_m) were possible only for relatively low gramicidin concentration (0, 0.1, 0.25, 1 μM) because at the higher gramicidin concentrations, membrane resistance is actually smaller than that of measuring electrodes and bathing solution resistance. To calculate the specific conductivity λ_m from measured membrane resistance Ω, we used the following formula:

$$\lambda_m = \frac{d}{\Omega\{2\pi R^2 [1 + \sqrt{1 - (r/R)^2}]\}},$$

where the term in square brackets is the bilayer area with a shape correction accounting for the presence of the tip of radius r. The values obtained for λ_m correspond well with optically measured values λ_m in the low ionophore concentration range (see Fig. 5).

Dependence of rise time on the conductivity of the bathing solution

Fig. 6 shows that the linear dependence of the rate constant, t^{-1}, on the conductivity of the bathing solution, λ_0 (cf. Ehrenberg et al., 1987), is retained in the presence of gramicidin; the slope is steeper, as predicted by Eq. 1. The slope is (6.9 ± 0.15) 10^6 s^{-1} Ωcm for membranes without gramicidin and (20.33 ± 0.33)10^6 s^{-1} Ωcm for gramicidin-containing membranes (5 μM in the outer bathing solution), respectively.

The results in Fig. 6 for the experiments without gramicidin can be treated by safely assuming that the membrane conductance in Eq. 1 can be neglected. The

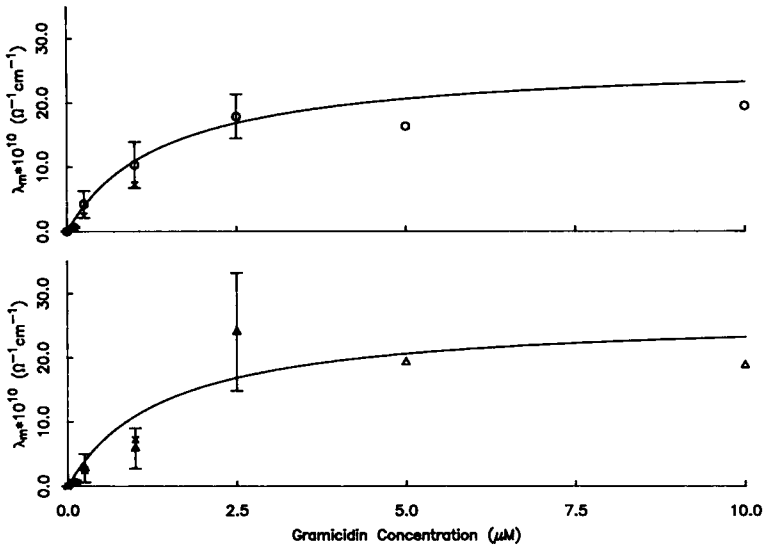

FIGURE 5 Gramicidin-induced variation in membrane electrical conductivity. The optical signal of di-4-ANEPPS can be used to calculate the conductivity of the SLB upon addition of gramicidin from the change in either the rate (O) or extent (△) of the fluorescence response to the applied field. The values obtained correspond well with electrically measured values (x) for the four gramicidin concentrations accessible to such measurements. The solid curve shown represents the result of fitting all data (O,△) with the same saturable one site binding equation.

only independently indeterminate parameter for the rate constant is then C_m. The value for C_m derived from the slope of the line in Fig. 6 is 0.64 $\mu F/cm^2$, which is closer to the value of 0.57 $\mu F/cm^2$ determined by Tien (1974) than the value of 0.71 in Ehrenberg et al. (1987), which was derived from data taken over a much smaller range of KCl concentrations. This value of C_m can then be used to analyze the data for the gramicidin-modified membrane via Eq. 1. Clearly, the conductivity of the membrane, λ_m must be proportional to the conductivity of the bathing solution, λ_o to account for the linear relationship with the steeper slope for the gramicidin data in Fig. 6. This proportionality implies that the individual channels are not saturated with ions at these electrolyte concentrations and that the molecular mechanism for migration through the channel is not especially different from simple diffusion. The proportionality constant obtained from the slope is 4×10^{-6}. This means that the conductance of a 50 Å membrane in equilibrium with 5 μM gramicidin is about equal to the conductance through a 1-mm-thick slab of electrolyte of the same surface area. This accounts for our inability to use direct electrical measurements to determine membrane resistance at the higher gramicidin concentration for the experiments associated with Fig. 5.

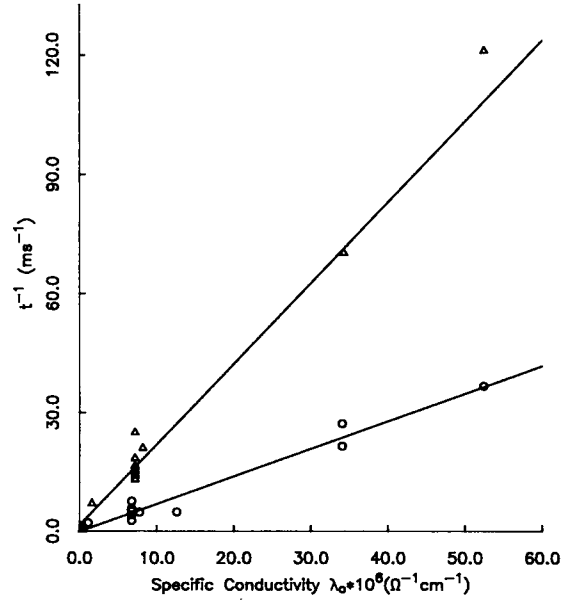

FIGURE 6 Linear dependence of bilayer charging rate on electrical conductivity of the bathing solution. (O) No gramicidin, (△) 5 μM of gramicidin in the bathing solution. The values from SLBs of various sizes were normalized to a radius of 1.5 mm.

DISCUSSION

The primary conclusion from this work is that Eq. 1 offers a good description of the membrane potential induced in a lipid bilayer membrane by an externally applied electric field, even when the membrane is modified to include ion channels. The fluorescence from a potentiometric dye afforded a direct measurement of the time course and the

amplitude of the induced potential. Both are modulated by changes in membrane or external medium conductivities and by the size of the spherical bilayer in ways that are quantitatively predictable with Eq. 1.

Because the induced potential varies along a surface and integrates to zero over the surface, potentiometric dyes are ideal tools for detailing the effects of externally applied fields on membranes. They permit the investigation of more complex geometries such as irregularly shaped cells and clumps of cells in contact (cf. Gross et al., 1986), where an analytical solution to Laplace's equation is not possible. Even for spherical cells, changes in the membrane permeability can lead to complex behavior which may yield to analysis with potentiometric dyes. For example, the movement of fluorescent markers after electroporation, can occur asymmetrically through localized regions of the membrane which have been variously identified as the pole facing the cathode (for red cell ghosts, see Sowers and Lieber, 1986) or the anode (for oat mesophyl protoplasts, see Mehrle et al., 1985). These puzzling results are representative of the open problems associated with the lack of a complete physical understanding of the process of dielectric breakdown (and its reversal). A potentiometric dye was employed in an elegant study of electroporation in sea urchin eggs (Kinosita et al., 1988).

It should also be possible to experimentally probe the more subtle effects of electric fields on cell physiology. Gross (1988) has recently completed a theoretical analysis of the modulation of the induced potential by a preexisting membrane surface potential. He shows that the redistribution of electromobile charged surface molecules (Jaffe and Nuccitelli, 1977; Poo, 1981) can produce major diminutions in the induced membrane potential over times ranging from minutes to hours. These ideas can be directly tested experimentally with the potentiometric dye approach and should have significant implications for our understanding of the subtle influence of extracellular fields in cell development and growth.

Eq. 1 is derived from the model of a uniform spherical shell in a uniform electric field. We felt it was important to test if this simple model does indeed apply to a lipid bilayer containing discrete ion channels and immersed in an aqueous electrolyte. The level of consistency between the theoretical model and the experimental data validates the assumptions made during earlier investigations of both slow and rapid effects of electric fields on cells, tissues, and organs.

We are pleased to thank the United States Public Health Service for their support of this work under grant GM35063.

Received for publication 27 June 1988 and in final form 14 March 1989.

REFERENCES

Andersen, O. S. 1984. Gramicidin channels. *Annu. Rev. Physiol.* 46:531–548.

Bates, G. W., J. J. Gaynor, and N. S. Shekhawat. 1983. Fusion of plant protoplasts by electric field. *Plant Physiol.* 72:1110–1113.

Chan, C. Y., and C. Nicholson. 1986. Modulation by applied electric fields of Purkinje and stellate cell activity in the isolated turtle cerebellum. *J. Physiol. (Lond.).* 371:89–114.

Ehrenberg, B., D. L. Farkas, E. N. Fluhler, Z. Lojewska, and L. M. Loew. 1987. Membrane potential induced by external electric field pulses can be followed with a potentiometric dye. *Biophys. J.* 833–837.

Farkas, D. L., R. Korenstein, and S. Malkin. 1984. Electrophotoluminescence and the electrical properties of the photosynthetic membrane I initial kinetics and the charging capacitance of the membrane. *Biophys. J.* 45:363–374.

Fluhler, E, V. G. Burnham, and L. M. Loew. 1985. Spectra, membrane binding and potentiometric responses of new charge shift probes. *Biochemistry.* 24:5749–5755.

Goldsworthy, A. 1986. Switched-on tissue cultures. *Trends Biotechnol.* 4:227–230.

Gross, D. 1988. Electromobile surface charge alters membrane potential changes induced by applied electric fields. *Biophys. J.* 54:879–884.

Gross, D., L. M. Loew, and W. W. Webb. 1986. Optical imaging of cell membrane potential changes induced by applied electric fields. *Biophys. J.* 50:339–348.

Hassner, A., D. Birnbaum, and L. M. Loew. 1984. Charge shift probes of memrane potential synthesis. *J. Org. Chem.* 49:2546–2551.

Jaffe, L. F., and R. Nuccitelli. 1977. Electrical controls of development. *Annu. Rev. Biophys. Bioeng.* 6:445–476.

Jaffe, L. F., and M.-M. Poo. 1979. Neurites grow faster towards the cathode than the anode in a steady field. *J. Exp. Zool.* 209:115–128.

Kagawa, Y., and T. Hamamoto. 1986. ATP formation in mitochondria, submitochondrial particles, and F_0F_1 liposomes driven by electric pulses. *Methods Enzymol.* 126:640–643.

Kinosita, K., I. Ashikawa, N. Saita, N. Yoshimura, H. Itoh, K. Nagayama, and A. Ikegami. 1988. Electroporation of cell membrane visualized under a pulsed-laser fluorescence microscope. *Biophys. J.* 53:1015–1019.

Knight, D., and P. F. Baker. 1982. The chromaffin granule proton pump and calcium-dependent exocytosis in bovine adrenal medullary cells. *J. Membr. Biol.* 68:107–140.

Lin-Liu, S., W. R. Adey, and M.-M. Poo. 1984. Migration of cell surface concanavalin A receptors in pulsed electric fields. *Biophys. J.* 45:1211–1218.

Loew, L. M. 1982. Design and characterization of electrochromic membrane probes. *J. Biochem. Biophys. Methods.* 6:243–260.

Loew, L. M., and L. Simpson. 1981. Charge shift probes of membrane potential: a probable electrochromic mechanism for ASP probes on a hemispherical lipid bilayer. *Biophys. J.* 34:353–365.

Mehrle, W., U. Zimmermann, and R. Hampp. 1985. Evidence for asymetrical uptake of fluorescent dyes through electro-permeabilized membranes of avena mesophyll protoplasts. *FEBS (Fed. Eur. Biochem. Soc.) Lett.* 185:89–94.

Nea, L. J., G. W. Bates, and P. J. Gilmer. 1987. Facilitation of electrofusion of plant protoplasts by membrane-active agents. *Biochim. Biophys. Acta.* 897:293–301.

Neumann, E., A. E. Sowers, and C. Jordan. 1988. Electroporation and Electrofusion in Cell Biology. Plenum Publishing Corp., New York.

Obaid, A. L., R. K. Orkand, H. Gainer, and B. M. Salzberg. 1985. Active calcium responses recorded optically from nerve terminals of the frog neurohypophysis. *J. Gen. Physiol.* 85:481–489.

Poo, M.-M. 1981. In situ electrophoresis of membrane components. *Annu. Rev. Biophys. Bioeng.* 10:245–276.

Robinson, K. R. 1985. The response of cells to electric fields: a review. *J. Cell Biol. 101:2023–2027.*

Ryan, T. A., J. Myers, D. Holowka, B. Baird, and W. W. Webb. 1988. Molecular crowding on the cell surface. *Science (Wash. DC).* 239:61–64.

Singh, S., and J. L. Katz. 1986. Scientific basis of electro-stimulation. *J. Bioelectr.* 5:285–327.

Sowers, A. E., and M. R. Lieber. 1986. Electropore diameters, lifetimes, numbers, and locations in individual erythrocyte ghosts. *FEBS (Fed. Eur. Biochem. Soc.) Lett.* 205:179–184.

Tien, H. T. 1974. Bilayer Lipid Membranes. Marcel Dekker, Inc., New York. 478–483.

Tsong, T. Y. 1983. Voltage modulation of membrane permeability and energy utilization in cells. *Biosci. Rep.* 3:487–505.

Vinkler, C., R. Korenstein, and D. L. Farkas. 1982. External electric field–driven ATP synthesis in chloroplasts: a slow, ATP-synthase dependent reaction. *FEBS (Fed. Eur. Biochem. Soc.) Lett.* 145:235–240.

Zimmerman, U. 1982. Electric field-mediated fusion and related electrical phenomena. *Biochim. Biophys. Acta.* 694:227–277.